Elastocaloric effect in Ti-Ni shape-memory wires associated with the B2 ↔ B19' and B2 ↔ R structural transitions

Daniel Soto-Parra, Eduard Vives, Lluís Mañosa, J. A. Matutes-Aquino, Horacio Flores-Zúñiga, and Antoni Planes

Citation: Appl. Phys. Lett. **108**, 071902 (2016); doi: 10.1063/1.4942009
View online: https://doi.org/10.1063/1.4942009
View Table of Contents: http://aip.scitation.org/toc/apl/108/7
Published by the American Institute of Physics

Elastocaloric effect in Ti-Ni shape-memory wires associated with the B2 ↔ B19' and B2 ↔ R structural transitions

Daniel Soto-Parra,[1,2] Eduard Vives,[1] Lluís Mañosa,[1] J. A. Matutes-Aquino,[2] Horacio Flores-Zúñiga,[3] and Antoni Planes[1]
[1]*Departament d'Estructura i Constituents de la Matèria, Facultat de Física, Universitat de Barcelona, Diagonal, 647, E-08028 Barcelona, Catalonia, Spain*
[2]*Centro de Investigaciones en Materiales Avanzados, S. C. Miguel de Cervantes 120, Complejo Industrial Chihuahua, 31109 Chihuahua, México*
[3]*Instituto Potosino de Investigación Científica y Tecnológica, Camino a la Presa San José 2005, Col. Lomas 4a, CP.78216, San Luis Potosí, México*

(Received 26 November 2015; accepted 1 February 2016; published online 16 February 2016)

We have studied the elastocaloric properties of Ti-Ni shape-memory wires subjected to specific heat treatments to decouple the B2 ↔ R transition from the B2 ↔ B19' one. The entropy values at moderate stresses (∼170 MPa) for the B2 ↔ B19' transition are remarkably high (in the range 60–80 J/kg K). However, in spite of the B2 ↔ R transition exhibits significantly lower entropy changes (∼12 J/kg K), the much smaller hysteresis of this transition gives rise to a larger reversible elastocaloric effect for low applied stresses. Therefore, the reversible elastocaloric strength associated with the B2 ↔ R is larger than the elastocaloric strength associated with the B2 ↔ B19' transition. © *2016 AIP Publishing LLC*. [http://dx.doi.org/10.1063/1.4942009]

Giant caloric effects are expected to occur near first-order phase transitions.[1,2] These transitions can be field induced, which involves the exchange of latent heat with the surroundings. Therefore, a large entropy change results when the field is applied or removed isothermally while an adiabatic variation of the field gives rise to a large temperature change. The field is any externally controlled quantity that couples to the order parameter of the considered phase transition. In shape-memory alloys, the martensitic transformation can be induced by the application of a uniaxial stress, and these alloys are thus good candidates to display large caloric response upon loading and unloading. This is the elastocaloric effect that has recently attracted a lot of attention due to its potential interest for solid state refrigeration applications.[3] Elastocaloric properties of a number of shape-memory materials have been reported recently, including Cu-based,[4,5] Ti-Ni-based,[6,7] Fe-Pd,[8] and a number of magnetic shape memory alloys.[9,10] Furthermore, simple demonstrator cooling devices based on the elastocaloric effect have already been designed and tested.[11,12]

In the present paper, we study elastocaloric properties of commercial Ti-Ni wires (Dynalloy, Inc.). Ti-Ni is the most important shape-memory alloy owing to its exceptional mechanical properties.[13] It was discovered in the early sixties[14] and has been studied intensively for more than fifty years. This alloy displays shape-memory properties related to a thermoelastic martensitic transformation and has been used in many well established applications in diverse industrial fields.[15] Depending on thermomechanical treatments, the parent cubic B2 ($Pm\bar{3}m$) phase transforms to the monoclinic B19' ($P2_1/m$) martensitic phase either directly or in two steps via a first-order transition to the intermediate trigonal (P3) R-phase.[16] While the one step transformation path occurs in alloys quenched from high temperature, the two step path B2 → R → B19' happens in alloys containing Ti_3Ni_4 precipitates induced, for instance, by means of an intermediate temperature heat treatment. The transition to the B19' phase is responsible, to a large extent, for the interesting shape memory properties of Ti-Ni alloys, and the occurrence of the R-phase is usually seen as an undesirable feature.

Compared to the B2 ↔ B19', the B2 ↔ R transformation occurs with much little hysteresis and displays tremendous cycling stability. This suggests that in spite of a lower latent heat, interesting elastocaloric properties could arise associated with the B2 ↔ R transformation due to a better reversibility. The aim of the present paper is to compare elastocaloric properties in the vicinity of the B2 ↔ B19' and B2 ↔ R transitions. For such purpose, we have performed calorimetric and mechanical measurements on Ti-Ni wires that transform either directly from B2 to the B19'-phase or in two steps via an intermediate R-phase. While most of the studies on the elastocaloric effect in Ti-Ni have focussed in measuring temperature changes in wires and thin films induced by the adiabatic (fast) loading and unloading superelastic cycles, there is a lack of information on the entropy change associated with the elastocaloric effect in this alloy. In the present paper, we provide data for the entropy change characterizing the elastocaloric effect associated with B2 to R and B2 to B19' transitions of commercial Ti-Ni wires subjected to moderate uniaxial stresses.

The composition of the studied wires was determined to be $Ti_{52.6}Ni_{47.4}$ from EDX analysis. Samples for tensile experiments were first heat treated at 883 K for 30 min and then quenched in a mixture of ice and water (we will denote this heat treatment *HT*1). After this heat treatment, the B2-phase directly transforms to the B19'-phase on further cooling. In order to decouple the transition to the R-phase from the transition to the B19'-phase, the heat treatment was performed at 773 K (denoted *HT*2) instead of 883 K. We have carried out DSC measurements on samples subjected to *HT*1 and *HT*2 heat treatments aimed at determining (in the absence of applied stress) transition entropy changes and

characteristic temperatures [M_s (A_s) and M_f (A_f) are the temperatures at which the forward to the B19' phase (reverse to the B2 phase) transition starts and finishes, respectively. R_s and R_f are the corresponding temperatures for the forward B2 → R transition]. The obtained values are given in Figs. 1(a) and 1(b), which show examples of DSC curves obtained for both heat treatments. Note that for the sample subjected to the *HT*2 treatment, the forward transition occurs in two steps, B2 → R → B19', while the reverse transition occurs directly from the B19'-phase to the B2-phase. However, if the temperature rate is reversed before the R → B19' transition occurs, the reverse R → B2 transition occurs with very weak hysteresis [see the inset of Fig. 1(b)]. It is worth noting that $|\Delta S(B2 \rightarrow R) + \Delta S(R \rightarrow B19')| = |\Delta S(B19' \rightarrow B2)|$ within the errors. Note that the obtained results are in agreement with the previously published data (see, for instance, Ref. 17).

With the aim of quantifying elastocaloric properties of TiNi-wires, changes of entropy induced by isothermal application of stress have been determined from measurements of sample elongation, L (obtained as the difference $l - l_0$, where l is the actual length and l_0 is the sample gauge at room temperature and zero applied force), as a function of temperature, T, during the thermally induced martensitic transition under constant applied uniaxial force. For these experiments, we used wires of sample gauge, $l_0 \simeq 37.5$ mm and cross-section $\phi \simeq 0.195$ mm^2.

Experiments were performed in a force-controlled machine equipped with a cryofurnace that enables a good control of the temperature (measured within ±1 K). The force is applied by hanging a dead load from the lower grip at which the wire is attached and was monitored with a load cell with a resolution of ∼1 N in the range of kN.[18] Sample elongation was measured with a strain gauge extensometer attached to the sample. Initially, the sample was heated up above the A_f temperature. Then, a selected tensile force was applied and the sample was cooled down at a rate of 1 K/min. The measurement protocol is schematically depicted in Fig. 2 and explained in its caption for the case of samples subjected to *HT*1 and *HT*2 heat treatments. In the figure, symbols correspond to the temperature of the inflection point on the measured L vs. T curves, which provide a good estimation of the transition temperatures as a function of the applied stress. Note that while the hysteresis of the B2 ↔ B19' transition is ∼40 K, the B2 ↔ R transition occurs with a narrower hysteresis of ∼5 K, almost independent of the applied stress.

L against T curves obtained by cycling within the region of the B2 → B19' → B2 and B2 → R → B2 transitions in samples subjected to heat treatments *HT*1 and *HT*2, respectively, were obtained. Examples of L vs. T curves at selected applied stress (estimated as F/ϕ) for the forward B2 ↔ B19' and B2 ↔ R transitions are shown in Figs. 3(a)–3(d). Note that increasing the stress shifts the elongation curves to higher temperatures due to the expected increase of stability of the martensitic phase. The corresponding increase of

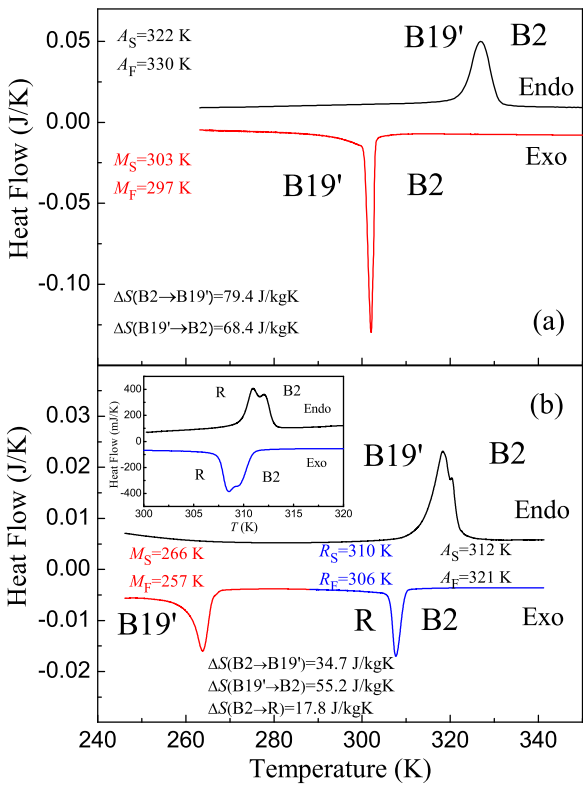

FIG. 1. Calorimetric measurements after *HT*1 (a) and *HT*2 (b) heat treatments. The inset in panel (b) shows a calorimetric run after a *HT*2 heat treatment, where the temperature rate has been reversed before the R → B19' occurs.

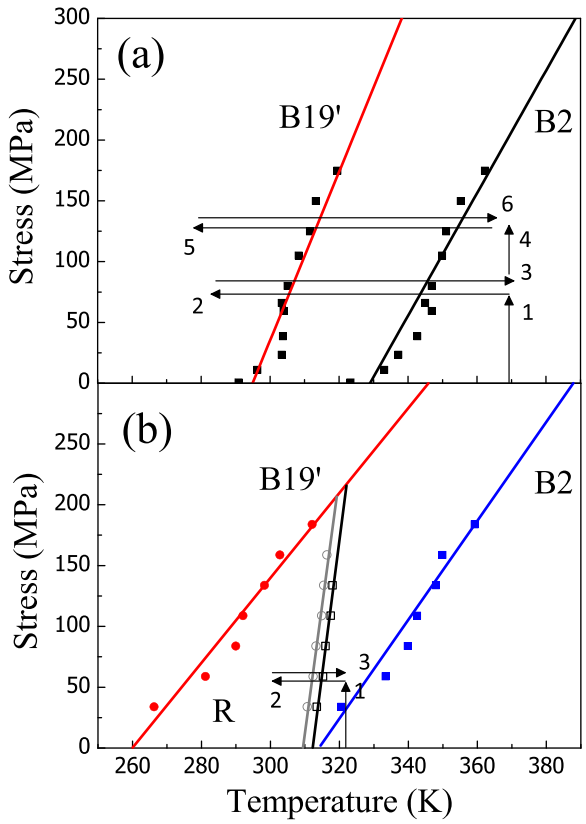

FIG. 2. Transition temperatures as a function of the applied stress after *HT*1 (a) and *HT*2 (b) heat treatments. The protocol followed to measure L vs. T curves at selected applied stresses is indicated in each case with arrows. The sample is first heated up above A_f, then a given force is applied (1), and the sample is cooled down below M_f or R_f (2) and heated up above the corresponding reverse transition (3). The force is then increased (4), and the sample is thermally cycled across the studied transition: (4) → (5) → (6).

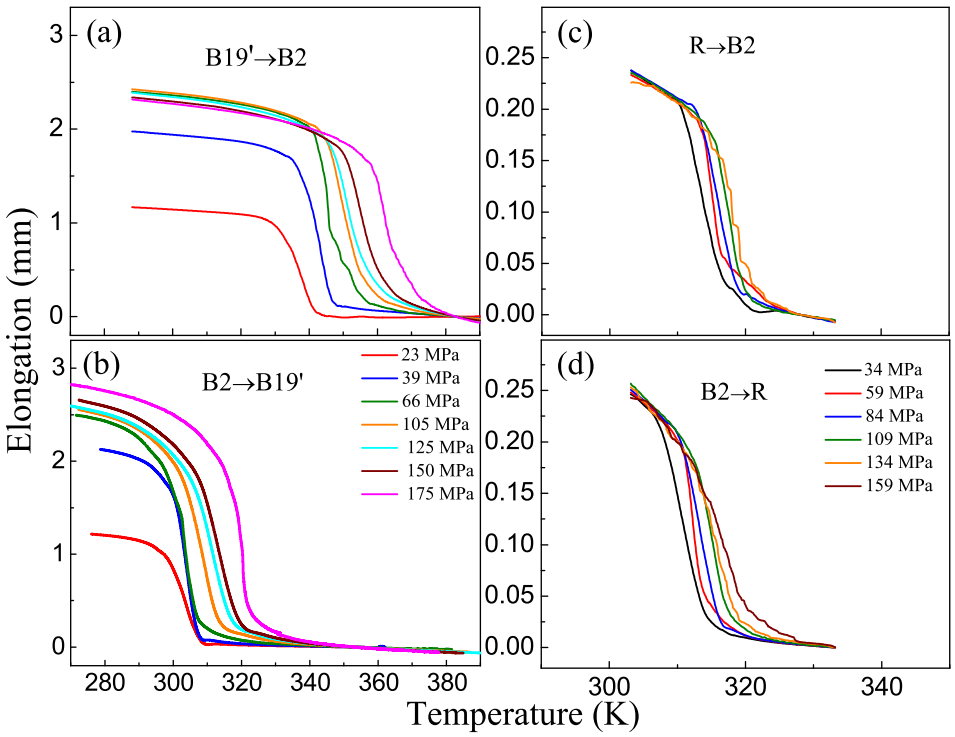

FIG. 3. Examples of L vs. T curves at selected applied stresses for the B19' → B2 (a), B2 → B19' (b), R → B2 (c), and B2 → R (d) transitions.

elongation is a consequence of the fact that stress breaks the degeneracy associated with the symmetry-allowed martensitic variants that are equivalent in the absence of stress. Therefore, within each grain, the increase of the uniaxial stress gives rise to a gradual increase in the fraction of martensitic variants which are crystallographically oriented in a direction energetically favorable to its the direction, thus giving rise to an increase of elongation.

Isothermal force-induced entropy changes, $\Delta S(T,F)$, have been computed from L vs. T curves taking into account that

$$\Delta S(T,F) = \frac{1}{m}\int_0^F \left(\frac{\partial L}{\partial T}\right)_F dF, \qquad (1)$$

where the Maxwell relation, $(\partial S/\partial F)_T = (\partial L/\partial T)_F$, has been used ($m$ is the sample mass). The entropy vs temperature curves for the B2 → B19' and B19' → B2 transitions in a sample subjected to a *HT*1 treatment are shown in Fig. 4. The corresponding curves for the B2 → R and R → B2 transitions in a sample subjected to a *HT*2 treatment are shown in Fig. 5. In Ti-Ni, application of stress stabilizes the low temperature phase (with a large strain), as cooling does, which results in a decrease of entropy thereby giving rise to a conventional caloric effect. The entropy values found for the B2 → B19' transition are remarkably high, even for moderate stresses of 175 MPa, and are among the highest values reported for any caloric material.[2] For the B2 → R transition, the entropy values are smaller but still within the range of those reported for other giant caloric materials.

For operational purposes, the reversibility of a caloric effect under cyclic application of the external load is a key parameter. The reversibility of the elastocaloric effect near a first-order structural phase transition crucially depends on the competition between the width of thermal hysteresis and the sensitivity of transition temperatures upon an applied external force/stress. A narrow hysteresis and a large shift of transition temperatures with the applied stress favours reversibility. For a given hysteresis, substantial reversibility occurs when the stress-induced shift of the whole hysteresis loop is larger than thermal hysteresis. However, in general, this requires application of very large stresses. In the case of

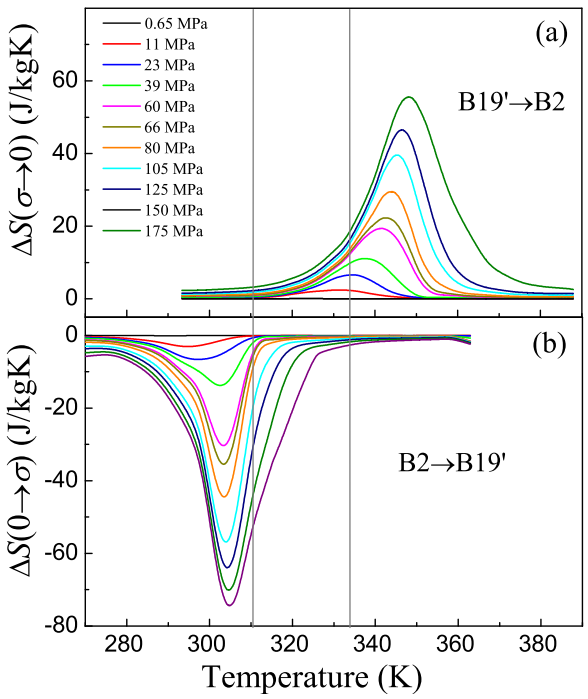

FIG. 4. Isothermal force-induced entropy change quantifying the elastocaloric effect in the vicinity of the B2 ↔ B19' transition as a function of temperature and selected values of the applied stress in a sample subjected to a *HT*1 heat treatment. (a) Reverse transition: the entropy change is computed for $\sigma \rightarrow 0$ stress removal. (b) Forward transition: the entropy change is computed for $0 \rightarrow \sigma$ stress application. Vertical lines indicate the reversible region.

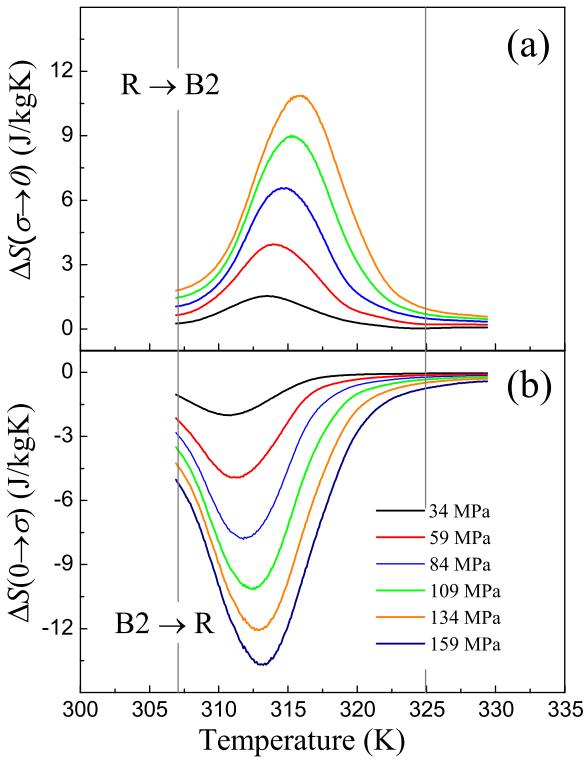

FIG. 5. Isothermal force-induced entropy change quantifying the elastocaloric effect in the vicinity of the B2 ↔ R transition as a function of temperature and selected values of the applied stress in a sample subjected to a *HT*1 heat treatment. (a) Reverse transition: the entropy change is computed for $\sigma \rightarrow 0$ stress removal. (b) Forward transition: the entropy change is computed for $0 \rightarrow \sigma$ stress application. Vertical lines indicate the reversible region.

the magnetocaloric effect, a reversible contribution has been shown to occur within a temperature interval bounded by the start of the forward transition on cooling at zero applied magnetic field and the start of the reverse transition under an applied field.[19,20] Actually, in this temperature region, the magnetic field carries the state of the material through a minor hysteresis loop, and the reversibility in the magnetocaloric effect is directly related to the reversibility in the fraction of material that undergoes the forward and reverse transitions in the cycle. Here, we assume that the same result applies in the case of the elastocaloric effect, and we determine the reversible component of the elastocaloric effect assuming that it is also related to the reversibility in the fraction of material that undergoes the forward and reverse transition in the cycle under application and removal of the force/stress. With this idea in mind, we have obtained the reversible component of the elastocaloric effect associated with the B2 ↔ B19' and B2 ↔ R transitions from the results depicted in Figs. 4 and 5, respectively, where reversibility is expected within the temperature range bounded by the two vertical lines. In Fig. 6, we have plotted the maximum value of the reversible stress-induced entropy change for the B2 ↔ B19' and B2 ↔ R transitions as a function the applied stress. In the studied range of applied stresses, the temperature interval of reversibility is similar (∼10 K for the B2 ↔ B19' transition and ∼15 K for the B2 ↔ R transition), but the reversible elastocaloric strength (estimated from the mean slope of the curves depicted in Fig. 6) for B2 ↔ R transition is more than twice that for the B2 ↔ B19' transition.

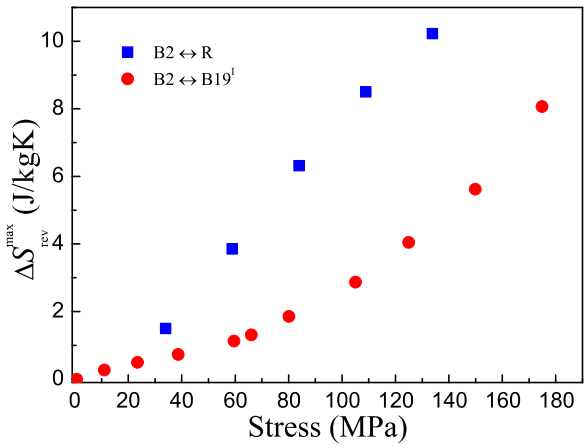

FIG. 6. Maximum value of the reversible entropy change for the B2 ↔ B19' (red circles) and for the B2 ↔ R (blue squares) transitions as a function of the applied stress.

Finally, we would like to mention that present results have been obtained during the early stages of thermal cycling under applied stress of the materials. Since degradation of the superelastic behaviour is known to occur during successive cycling,[21] we expect that these results could be affected by further cycling. In any case, we foresee that the B2 ↔ R transition should be much less affected by cycling than the B2 ↔ B19' transition due to its higher reversibility.

To summarize, in the present paper, we have studied elastocaloric properties of Ti-Ni shape memory wires associated with the B2 ↔ B19' and B2 ↔ R transitions. The transition to the R-phase has been decoupled from the direct transition to the B19'-phase by means of an appropriate heat treatment. While a very high entropy change of more than 60 J/kg K can be isothermally induced by the application of ∼175 MPa associated with the B2 → B19' transition, which is almost one order of magnitude larger than the entropy change induced in the vicinity of the B2 → R transition for a similar stress, the reversible component of this last transition is larger than the reversible component associated with the B2 ↔ B19' transition. This result nicely illustrates the fact that for an optimal elastocaloric effect in the vicinity of a first-order phase transition, an adequate balance between the amount of latent heat and the thermal hysteresis extension must be achieved in order to reach a maximum reversible elastocaloric strength.

We acknowledge financial support from the Spanish Ministry of Science, Project No. MAT2013-40590-P.

[1]L. Mañosa, A. Planes, and M. Acet, J. Mater. Chem. A **1**, 4925–4936 (2013).
[2]X. Moya, S. Kar-Narayan, and N. D. Mathur, Nat. Mater. **13**, 439 (2014).
[3]J. Tušek, K. Engelbrecht, R. Millán-Solsona, L. Mañosa, E. Vives, L. P. Mikkelsen, and N. Pryds, Adv. Energy Mater. **5**, 1500361 (2015).
[4]E. Bonnot, R. Romero, L. Mañosa, E. Vives, and A. Planes, Phys. Rev. Lett. **100**, 125901 (2008).
[5]L. Mañosa, S. Jarque-Farnos, E. Vives, and A. Planes, Appl. Phys. Lett. **103**, 211904 (2013).
[6]J. Cui, Y. Wu, J. Muehlbauer, Y. Hwang, R. Radermacher, S. Fackler, M. Wuttig, and I. Takeuchi, Appl. Phys. Lett. **101**, 073904 (2012).
[7]H. Ossmer, F. Lambrecht, M. Gültig, C. Chluba, E. Quandt, and M. Kohl, Acta Mater. **81**, 9–20 (2014).

[8]F. Xiao, T. Fukuda, and T. Kakeshita, Appl. Phys. Lett. **102**, 161914 (2013).
[9]R. Millán-Solsona, E. Stern-Taulats, E. Vives, A. Planes, J. Sharma, A. K. Nayak, K. G. Suresh, and L. Mañosa, Appl. Phys. Lett. **105**, 241901 (2014).
[10]Y. Xu, B. Lu, W. Sun, A. Yan, and J. Liu, Appl. Phys. Lett. **106**, 201903 (2015).
[11]M. Schmidt, A. Schütze, and S. Seelecke, Int. J. Refrig. **54**, 88 (2015).
[12]H. Ossmer, S. Miyazaki, and M. Kohl, in *Proceedings of the 18th International Conference on Solid-State Sensors, Actuators and Microsystems, Transducers* (2015), p. 726.
[13]K. Otsuka and X. Ren, Prog. Mater. Sci. **50**, 511–678 (2005).
[14]W. J. Buehler, J. V. Gilfrich, and R. C. Wiley, J. Appl. Phys. **34**, 1475 (1963).
[15]"Science and Technology of Shape-Memory Alloys: New Developments," in *MRS Bulletin*, edited by K. Otsuka and T. Kakeshita (Mater. Res. Soc., 2002), Vol. 27, p. 2.
[16]Crystallography, thermomechanical properties, and the effect of heat treatments on Ti-Ni-based shape-memory alloys have been discussed in detail in Ref. 13. As explained in that reference, for some compositions and doping, as for instance in Cu-doped TiNi, the B2 phase transforms via a B19 (Pmma) structure.
[17]G. Fan, W. Chen, S. Yang, J. Zhu, X. Ren, and K. Otsuka, Acta Mater. **52**, 4351–4362 (2004).
[18]A similar machine has been described in E. Bonnot, R. Romero, X. Illa, L. Mañosa, A. Planes, and E. Vives, Phys. Rev. B **76**, 064105 (2007).
[19]I. Titov, M. Acet, M. Farle, D. Gonzàlez-Alonso, L. Mañosa, A. Planes, and T. Krenke, J. Appl. Phys. **112**, 073914 (2012).
[20]E. Stern-Taulats, P. O. Castillo-Villa, L. Mañosa, C. Frontera, S. Pramanick, S. Majumdar, and A. Planes, J. Appl. Phys. **115**, 173907 (2014).
[21]J. Tušek, K. Engelbrecht, L. P. Mikkelsen, and N. Pryds, J. Appl. Phys. **117**, 124901 (2015).